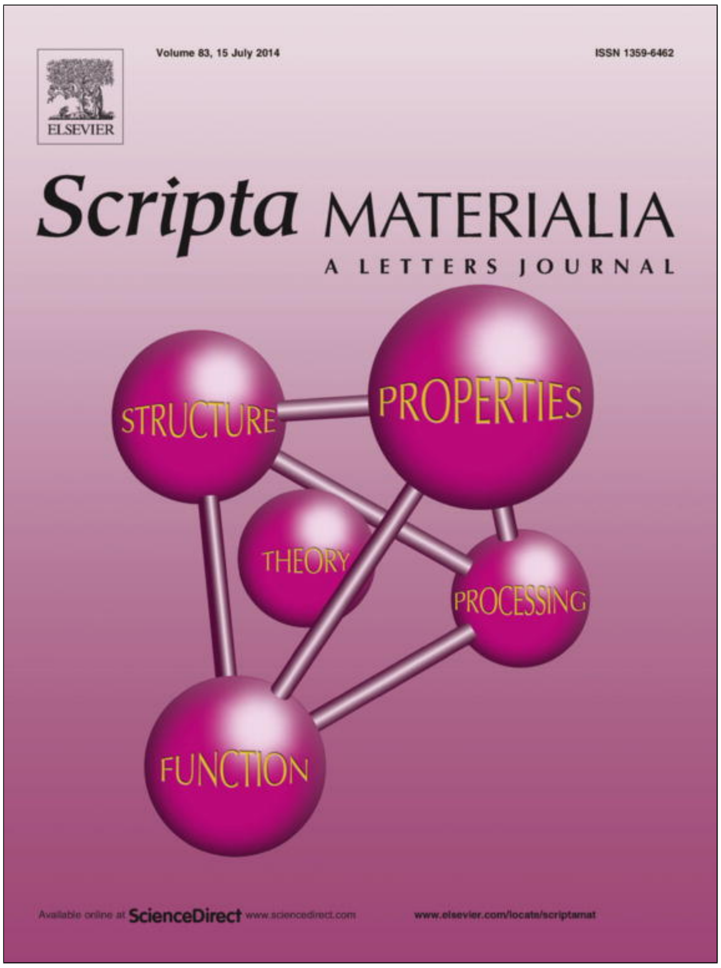
Volume 83, 15 July 2014
ISSN 1359-6462
ELSEVIER
Scripta MATERIALIA
A LETTERS JOURNAL
STRUCTURE
PROPERTIES
THEORY
PROCESSING
FUNCTION
Available online at ScienceDirect www.sciencedirect.com
www.elsevier.com/locate/scriptamat

Available online at www.sciencedirect.com
ScienceDirect
Scripta Materialia 83 (2014) 17–20
Scripta MATERIALIA
www.elsevier.com/locate/scriptamat

Strengthening zones in the Co matrix of WC–Co cemented carbides

I. Konyashin,[a,g] F. Lachmann,[a] B. Ries,[a] A.A. Mazilkin,[b,c] B.B. Straumal,[b,d,e,*] Chr. Kübel,[d] L. Llanes[f] and B. Baretzky[d]

[a]*Element Six Hard Materials, Element Six GmbH, 36151 Burghaun, Germany*
[b]*Institute of Solid State Physics, Russian Academy of Sciences, 142432 Chernogolovka, Russia*
[c]*Max-Planck-Institut für Intelligente Systeme, Heisenbergstrasse 3, 70569 Stuttgart, Germany*
[d]*Karlsruher Institut für Technologie, Institut für Nanotechnologie, 76344 Eggenstein-Leopoldshafen, Germany*
[e]*Moscow Institute of Physics and Technology (State University), Institutskii per. 9, 141700 Dolgoprudny, Russia*
[f]*Universitat Politecnica de Catalunya, Av. Diagonal, 647, 08028 Barcelona, Spain*
[g]*National University of Science and Technology MISIS, Leninsky Prospect, 4, 119049 Moscow, Russia*

Received 24 November 2013; revised 31 March 2014; accepted 31 March 2014
Available online 5 April 2014

For conventional structural and tool materials, in particular WC–Co cemented carbides, hardness and wear-resistance can usually be increased only at the expense of toughness and strength. For the first time we have achieved a dramatically increased combination of hardness, wear-resistance, fracture toughness and strength as a result of precipitation of extremely fine nanoparticles in the cobalt binder of cemented carbides. These nanoparticles are ~3 nm in size, coherent with the Co matrix and consist of a metastable phase.

Keywords: Cemented carbides; Toughness; Strength; Nanoprecipitates

WC–Co cemented carbides are metal–ceramic composites consisting of a ceramic phase, tungsten carbide and a cobalt binder. They are widely used in various industrial applications as well as domestically (e.g. masonry drill bits) due to their high hardness, wear-resistance, toughness and strength. Since their discovery in Germany in the 1920s, WC–Co cemented carbides have not dramatically changed. The main improvements effected relate to varying WC grain size, Co content and employing inhibitors of WC grain growth during liquid-phase sintering [1,2]. However, attempts to strengthen the Co matrix have not up to now been successful. The state and hardness of binder interlayers play a decisive role with respect to the wear-resistance of the cemented carbides. The binder interlayers are found to be worn out very rapidly during operation leaving unsupported WC grains, which results in the low wear-resistance and short tool lifetime of the conventional cemented carbide as a whole [3]. Therefore, the major challenge of research in the carbide field is to improve the wear-resistance of cemented carbides significantly without sacrificing their strength and fracture toughness. Recently we developed and patented a novel approach to the fabrication of cemented carbides and elaborated a new generation of cemented carbides on the basis of this approach [4–8]. For the first time, we managed to obtain a dramatically improved combination of hardness, wear-resistance, fracture toughness and transverse rupture strength of WC–Co materials. The aim of this investigation is to reveal the structural reasons for this achievement.

Five cemented carbides were prepared, one according to Refs. [17,19] and four according to the new technology (see Table 1 for details). Metallographic sections of the samples were examined on a Zeiss LEO 438VP scanning electron microscope. Hardness (HV_{30}) measurements were carried out according to DIN ISO 3878 at a load of 300 N. The indentation fracture toughness K_{1C} was measured by the Palmqvist method at a load of 1000 N after annealing of the cross-sectional

* Corresponding author at: Institute of Solid State Physics, Russian Academy of Sciences, Chernogolovka, Moscow District 142432, Russia. Tel.: +7 916 6768673; fax: +7 499 2382326; e-mail: straumal@issp.ac.ru

http://dx.doi.org/10.1016/j.scriptamat.2014.03.026
1359-6462/

Table 1. Preparation of cemented carbides.

	Cemented carbide according to the Refs. [17,19]	Novel cemented carbides
Carbon content (converted values with respect to WC)	Very low, 5.75 wt.% C	Medium–low, 6 wt.% C
Starting WC powder	Grain size 1.4 μm, 6.12 wt.% C	Grain size 2.0, 2.7, 4.9, 5.0 μm, 6.12 wt.% C
Ball milling with	10 wt.% Co, 5.7 wt.% W	6.0, 10, 6.5 and 9.5 wt.% Co, 2 wt.% W
Sintering	1450 °C, 75 min in vacuum	1450 °C, 45 min in vacuum + 30 min HIP in Ar at 4 MPa
Post-annealing	800 °C, 20 h in vacuum	600 °C, 10 h in vacuum

samples in a vacuum at 800 °C for 60 min according to ISO/DIS28079. The fracture toughness $K_{1C(4)}$ was determined under four-point bending using single edge notched bend samples. Transverse rupture strength (TRS) was examined according to ISO 3327. Wear-resistance was examined according to ASTM B611-85 standard. Transmission electron microscopy (TEM, HRTEM, STEM, EDXS) studies were carried out on a TITAN 60-300 instrument. Tilting experiments were carried out on JEM-100CX microscope. The electron diffraction patterns were simulated using JEMS software written by P. Stadelmann [9].

It is well known that one can vary hardness, wear-resistance, strength and toughness of cemented carbides over a wide range by conventional approaches based on varying the Co content and WC mean grain size. However, their hardness and consequently wear-resistance can be increased only at the expense of fracture toughness [10,11]. The dependence of abrasion wear vs. fracture toughness of conventional WC–Co cemented carbides is represented by a relatively narrow hyperbolic band shown by the black curve in Figure 1. It is very difficult to escape from this band via conventional approaches, e.g. by employing WC nanopowders [12–14], carbon or inorganic nanotubes [15] or precipitation hardening of the Co binder [16–20].

Our newly developed technological procedure allowed us to produce fundamentally novel WC–Co cemented carbides containing ultra-coarse WC grains (see inset in Figure 1) and enhanced Co-based binder.

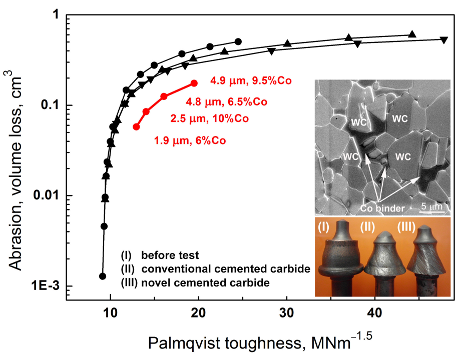

Figure 1. Baseline indicating the abrasion wear vs. fracture toughness for conventional WC–Co cemented carbides (black curves) [11] and the corresponding curve for the novel cemented carbides with various values of WC mean grain size and Co content (red curve). Insets: microstructure of the novel cemented carbide with 6.5% Co containing rounded WC grains with mean grain size of 4.8 μm and thick Co-based binder matrix among them (top). Typical road-planing picks before and after field testing (bottom).

The dependence of abrasion wear on the fracture toughness for the novel cemented carbides shown by the red curve in Figure 1 clearly indicates that we have been able to break out from the the hyperbolic dependence, which is inherent to conventional cemented carbides.

Table 2 lists the mechanical properties of the novel cemented carbide in comparison to conventional WC–Co with the same Co content and similar WC mean grain size but comprising the nanograin-reinforced binder. HV_{30} and TRS as well as the wear-resistance of the novel cemented carbide significantly increase without degradation of the fracture toughness, which can be compared with mechanical properties of different grades of conventional WC–Co cemented carbides [21–25].

The microstructure and morphology of WC grains of the conventional ultra-coarse WC–Co grade are characterized by faceted WC grains varying from nearly 2–10 μm in size which are described in detail in Ref. [26]. The structure of the novel cemented carbide comprised rounded WC grains varying from nearly 1–8 μm in size [6,26]. It contains very thick binder interlayers of Co among the WC grains (Fig. 2), which results in a very high level of Palmquist fracture toughness of >18 MPa $m^{1/2}$. The structure and phase composition of these Co binder interlayers are the object of the present study.

Figure 2 shows the structure of the binder in the cemented carbide made according to Refs. [17,19] (see Table 1). It has a very low carbon content and consequently a high concentration of tungsten dissolved in the binder. Ageing leads to the precipitation of nano-needles in the hexagonal close-packed (hcp) ε-Co matrix. These needles can be clearly seen in HRTEM and STEM images. The nano-needles of nearly 10–40 nm in diameter are densely distributed in the binder volume. They grow parallel to each other, forming a so-called "nano-brush". The needles are normal (Fig. 2a–c) or parallel to the plane of the picture (Fig. 2d–f). According to the results of HRTEM (Fig. 2c and f) and EDXS analysis (Fig. 2e) the needles have the same crystal structure and composition as the hard but brittle hexagonal intermetallic compound Co_3W (DO_{19} structure type). It can be seen from the TEM images that εCo and Co_3W phases are well aligned to each other and have the following orientation relationships: $[0001]_{\varepsilon Co}||[0001]_{Co_3W}$ and $[11\bar{2}0]_{\varepsilon Co}||[11\bar{2}0]_{Co_3W}$. We found that the precipitation of the nano-needles leads to a hardness increase of ∼10% in comparison to the initial state after sintering. However, the transverse rupture strength and fracture toughness of such cemented carbides significantly decrease by ∼15% and ∼25%, respectively. In this case, the binder is strongly embrittled and cannot effectively

Table 2. Comparison of mechanical properties of the novel cemented carbide and conventional grade with the same Co content of 6.5 wt.% and similar WC grain size.

	HV_{30}, GPa	TRS, MPa	Wear-resistance, $cm^3\ rev^{-1}$	K_{1C}, MPa $m^{1/2}$	$K_{1C(4)}$, MPa $m^{1/2}$	Mean tool lifetime, %	Mean breakage number, %
Conventional cemented carbide	11.0	2010	2.1×10^{-4}	17.7	16.6	100	100
Novel cemented carbide	11.3	2330	1.1×10^{-4}	18.2	16.1	190	80

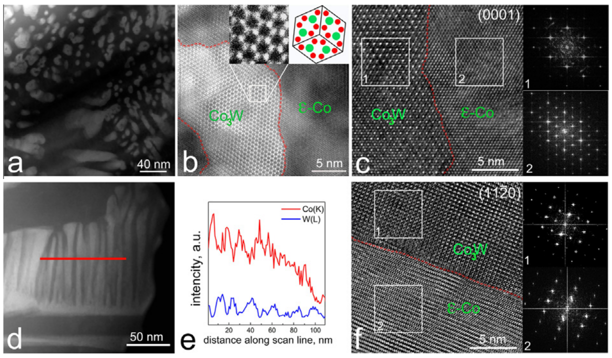

Figure 2. Structure of the binder in cemented carbide with low carbon content after conventional ageing: (a) STEM image of nano-needles, which are perpendicular to the plane of the picture; (b) HR STEM image of the nano-needle in (a). Two insets in (b) show an enlarged part of the needle and projection of the Co_3W cell along the (0001) axis, where the red and green spheres denote the positions of Co and W atoms, correspondingly. The position of the bright spots precisely coincides with that of the W atoms in the structure projection. (c) HRTEM image and corresponding fast Fourier transformation (FFT) patterns from the nano-needle of hexagonal (DO19) Co_3W surrounded by the εCo matrix (c2). (d) STEM image of the nano-needle parallel to the picture plane. (e) EDXS line-scan along the red line in (d) showing the variation of Co and W concentrations. (f) HRTEM image of the nano-needle as (d) and the corresponding FFTs from the εCo matrix (f1) and the hcp Co_3W nano-needle (f2). Red lines in (c) and (f) indicate the boundary between the Co_3W and the Co matrix.

prevent the propagation of cracks from WC grains during operation under impact loads. As a result, conventionally aged cemented carbides exhibit unacceptable performance in most mining and construction operations due to their low toughness and strength.

Due to our novel approach described in detail in Ref. [6] we have manufactured WC–Co cemented carbides with Co-based binder that are hardened and enhanced by nanoparticles (Table 1). The binder structure in the novel cemented carbide with 6.5 wt.% Co is shown in Figure 3. It consists of face-centered cubic (fcc) α-Co grains, which contain extremely fine nanoparticles with a mean grain size of ~3 nm. It can be seen from the figure that the reinforcing particles are densely and uniformly distributed in the binder volume and are isolated from each other (Fig. 3a), so that there is no binder embrittlement as in the case of the nano-needles described above. This structural feature is the reason why the material achieves significantly better combinations of wear-resistance and fracture toughness (red curve in Figure 1). The crystal lattice of nanoparticles is coherent with that of the Co matrix and there is no clear interface between them (Fig. 3c). In order to determine the crystal structure of the phase, tilting experiments were carried out. The electron diffraction

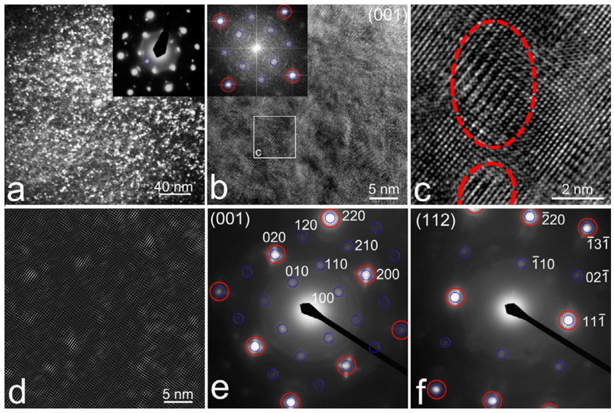

Figure 3. Structure of the binder in the novel cemented carbide: (a) dark-field TEM with the appropriate electron diffraction pattern (inset). The satellite reflection corresponding to the image in (a) arises from the nanoparticles and is marked by blue. (b,c) HRTEM images of nanoparticles embedded in the αCo matrix and the corresponding FFT pattern (inset in (b)), where the reflections from the nanoparticles are marked by blue and those from the αCo matrix are marked by red; two nanoparticles in (c) are marked by red circles. (d) The same as in (b) but after FFT filtering using the reflections from the nanoparticles to enhance their contrast. (e,f) Electron diffraction patterns from the αCo matrix containing the nanoparticles obtained by tilting towards two different crystal zones, i.e. (001) and (112), confirming that the nanoparticles have the cubic Cu_3Au lattice type. The red and blue circles indicate the location of the reflections in the simulated diffraction patterns from αCo and from the phase with the cubic Cu_3Au ($L1_2$) lattice type correspondingly. Red dashed lines in (c) indicate the phase particle locations.

patterns from the binder with the nanoparticles with αCo zone axes (114), (001) and (112) are shown in Figure 3a, e and f, respectively. According to the obtained data, the diffraction patterns from the precipitates are consistent with a Cu_3Au structure ($L1_2$ structure type). The simulated diffraction patterns of the Cu_3Au-type phase superimposed over the experimental electron diffraction pattern are shown as colored schemes in Figure 3e and f. The boundary between the phase and the matrix is fully coherent and they have the following orientation relationships: $[001]_{\alpha Co} \| [001]_{phase}$ and $[110]_{\alpha Co} \| [110]_{phase}$. Unfortunately it was not possible to determine the elemental composition of the particle because the spatial resolution of the TEM analysis is limited to the sample thickness (~50 nm), which is much larger than the particle size. According to numerous publications on the stable W–Co–C phase diagram [27], there is no stable phase with the Cu_3Au crystal lattice, so that the observed phase is metastable. The result obtained is in a good agreement with Ref. [18] where a metastable phase with a Cu_3Au structure was also found as a result of heat treatments of WC–Co materials.

The strengthening of solid solutions by natural and artificial ageing leading to the formation of coherent and semicoherent particles of metastable phases is widely used for the Al-based alloys [28]. This idea goes back to the invention of duralumin by Wilm [29], and explained later by Guinier [30] and Preston [31]. Nevertheless, the hardening method based on the precipitation of coherent nanoparticles of a metastable phase in a metallic binder has never previously been employed for metal–ceramic composites.

The novel nanostructured cemented carbides can be applied in construction, particularly in road building. For example, the machines used to remove worn and defective surface layers of asphalt or concrete from roads use a system comprising of ~200 picks with cemented carbide tips. The wear-resistance is increased and consequently tool lifetime is prolonged by a factor of ~2–3 when using the novel cemented carbide instead of the conventional material (Table 1). This is accompanied by a noticeable decrease in the number of pick breakages. Typical picks before and after field testing on asphalt-cutting are shown in the inset in Figure 1, and provide clear evidence that wear is dramatically reduced as a result of the enhancement of the cemented carbide binder. It was established that the grain size, morphology and crystal structures of the nanoparticles enhancing the binder phase remained unchanged during operation at elevated temperatures and high-impact loads during road-planing operations. These novel cemented carbides with nano-enhanced binder are currently manufactured on a large scale: more than one million road-planing picks with tips of the novel cemented carbide are produced annually.

We conclude that for conventional cemented carbides, the hardness and wear-resistance can be increased only at the expense of toughness and strength. In this work a dramatically increased combination of hardness, wear-resistance, fracture toughness and strength has been achieved. This is a result of the precipitation of extremely fine nanoparticles in the Co binder of cemented carbides. These nanoparticles are ~3 nm in size, coherent with the Co matrix and consist of a metastable phase. These novel cemented carbides belong to a new class of hard materials and are the only industrial nanostructured cemented carbides currently being fabricated anywhere in the world.

The authors gratefully acknowledge the support from the Karlsruhe Nano Micro Facility and the Ministry of Education and Science of the Russian Federation in the framework of the Increase Competitiveness Program of MISIS.

[1] A. Bose, Int. J. Powder Met. 47 (2011) 31.
[2] H. Kolaska, Powder Met. Int. 24 (1992) 311.
[3] I. Konyashin, F. Schäfer, R. Cooper, B. Ries, J. Mayer, T. Weirich, Int. J. Refract. Met. Hard Mater. 23 (2005) 225.
[4] I. Konyashin, R. Cooper, B. Ries (Element Six) German patent 10258537 (2006).
[5] I. Konyashin, R. Cooper, B. Ries (Element Six) European patent 1520056 (2004).
[6] I. Konyashin, B. Ries, F. Lachmann (Element Six) European patent WO2012/130851 (2012).
[7] I. Konyashin, B. Ries, F. Lachmann (Element Six) USA patent US2006/0093859 (2006).
[8] I. Konyashin, B. Ries, F. Lachmann (Element Six) European patent WO2012/004292 (2012).
[9] http://cimewww.epfl.ch/people/stadelmann/jemsWebSite/jems.html.
[10] B. Roebuck, M.G. Gee, R. Morrell, in: Proceedings 15th International Plansee Seminar 4, 2001, p. 245.
[11] W.D. Schubert, H. Neumeister, G. Kinger, B. Lux, Int. J. Refract. Met. Hard Mater. 16 (1998) 133.
[12] Z. Fang, X. Wang, T. Ryu, K.S. Hwang, H.Y. Sohn, Int. J. Refract. Met. Hard. Mater. 27 (2009) 288.
[13] G.K. Shao, X.L. Duan, J.R. Xie, X.H. Yu, W.F. Zhang, R.Z. Yuan, Rev. Adv. Mater. Sci. 5 (2003) 281.
[14] I. Konyashin, B. Ries, F. Lachmann, Int. J. Refract. Met. Hard Mater. 28 (2010) 489.
[15] Y. Zhang, G. Zhan, X. Sheng, A.W. Lockstedt, A. Griffo, Y. Shen, H. Deng, M.K. Keshavan, USA patent application US2008179104A (2008).
[16] H. Suzuki, M. Sugiyama, T. Umeda, J. Jpn. Inst. Met. 28 (1964) 287.
[17] H. Suzuki, H. Kubota, Planseeber. Pulvermet. 14 (1966) 96.
[18] H. Jonsson, B. Aronsson, J. Inst. Met. 97 (1969) 281.
[19] D.L. Tillwick, I. Joffe, J. Phys. D 6 (1973) 1585.
[20] H. Grewe, J. Kolaska, Metallurgie 7 (1981) 563.
[21] I. Konyashin, B. Ries, F. Lachmann, Int. J. Refract. Met. Hard. Mater. 28 (2010) 489.
[22] I. Konyashin, B. Ries, F. Lachmann, R. Cooper, A. Mazilkin, B. Straumal, Inorg. Mater. Appl. Res. 2 (2011) 19.
[23] I. Konyashin, B. Ries, F. Lachmann, R. Cooper, A. Mazilkin, B. Straumal, A. Aretz, Int. J. Refract. Met. Hard. Mater. 26 (2008) 583.
[24] I. Konyashin, T. Eschner, F. Aldinger, V. Senchihin, Z. Metallkd 90 (1999) 403.
[25] I. Konyashin, A. Anikeev, V. Senchihin, V. Glushkov, Int. J. Refract. Met. Hard. Mater. 14 (1996) 41.
[26] I. Konyashin, Cemented carbides for mining, construction and wear parts, in: V. Sarin (Ed.), Comprehensive Hard Materials, Elsevier, Amsterdam, 2014, pp. 425–452.
[27] C.M. Fernandes, A.M.R. Senos, Int. J. Refract. Met. Hard Mater. 29 (2011) 405.
[28] S.P. Ringer, K. Hono, Mater. Character. 44 (2000) 101.
[29] A. Wilm, Metallurgie 8 (1911) 225.
[30] A. Guinier, Nature 142 (1938) 569.
[31] G.D. Preston, Nature 142 (1938) 570.